ELSEVIER

Journal of Chromatography A, 776 (1997) 255–273

JOURNAL OF CHROMATOGRAPHY A

Identification of hexahydroimidazo[1,2-*a*]pyrazine-3,6-diones and hexahydroimidazo[1,2-*a*]imidazo[1,2-*d*]pyrazine-3,8-diones, unusual products of silica-catalyzed amino acid thermal condensation and products of their thermal decomposition using coupled high-performance liquid chromatography–particle beam mass spectrometry and gas chromatography–Fourier transform infrared spectroscopy–mass spectrometry

Vladimir A. Basiuk*, Rafael Navarro-González

Laboratorio de Química de Plasmas y Estudios Planetarios, Instituto de Ciencias Nucleares, Universidad Nacional Autónoma de México, Circuito Exterior C.U., A. Postal 70-543, 04510 Mexico, D.F., Mexico

Received 23 December 1996; revised 21 March 1997; accepted 24 March 1997

Abstract

Sublimation of simple aliphatic amino acids (Ala, Aib, Val and Leu) at 230–250°C under reduced pressure in the presence of silica as a catalyst yields cyclic dipeptides piperazine-2,5-diones as major products. In addition, two types of unusual products have been detected. To determine their structures, we utilized a coupled HPLC–particle beam-MS and GC–Fourier transform IR–MS technique with auxiliary computer simulation of IR spectra. Based on the spectral data obtained, we identified the condensation products as substituted bicyclic and tricyclic amidines, hexahydroimidazo[1,2-*a*]pyrazine-3,6-diones and hexahydroimidazo[1,2-*a*]imidazo-[1,2-*d*]pyrazine-3,8-diones. Other peaks in the chromatograms has been identified as products of the amidines thermal decomposition. The general decomposition pattern includes dehydrogenation as well as cleavage of the carbon skeleton. The last process primarily affects the 6-membered pyrazine ring causing elimination of CO or HNCO, or/and the loss of α-substituents without or with α-carbon atom.

Keywords: Amino acid condensation; Amidines; Hexahydroimidazopyrazinediones

1. Introduction

Coupling gas chromatography (GC) and high-performance liquid chromatography (HPLC) with Fourier transform infrared spectroscopy (FTIR) and mass spectrometry (MS) affords highly powerful and reliable tools for analytical chemistry. Due to the use of GC–MS, GC–FTIR, GC–FTIR–MS, HPLC–MS, etc., impressive advances have been achieved in the separation and unambiguous identification of complex mixtures of organic compounds; for recent reviews, see for example Refs. [1–5]. The most

*Corresponding author.

0021-9673/97/$17.00
PII S0021-9673(97)00331-2

efficient, especially for the analysis of unknown compounds, is the simultaneous coupling of chromatography with FTIR and MS detectors (in series or in parallel), when obtaining both types of spectra allows even stereoisomers to be distinguished.

One of the applications where the hyphenated GC–MS technique appears indispensable is the analysis of peptide and protein pyrolyzates [6–11]. The tasks which were attempted using this method are rather versatile, from peptide and protein sequencing to the comparison of human hair pyrolytic patterns associated with criminal investigations. One of the most important findings observes that pyrolytic cleavage of long peptide chains with simultaneous cyclization of the dipeptide fragments formed [6,8,10,11], as well as thermal cyclocondensation of linear dipeptides [9], results primarily in the formation of cyclic dipeptides piperazine-2,5-diones (PDs).

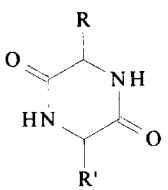

PD

A few years ago [12] we developed a novel synthetic method for direct dehydration of simple aliphatic amino acids to symmetric PDs (R=R′) by means of amino acid sublimation in the presence of silica as a catalyst under 170–220°C and reduced pressure. This approach was possible due to the finding by Gross and Grodsky [13] that simple amino acids can be sublimed in vacuo without appreciable decomposition and loss of optical activity. Under the strong dehydrating conditions of the method, PDs form in high yields. Thus, our task was an exclusively synthetic one, contrary to the "destructive" goal of the pyrolytic methods. Nevertheless, it has a certain relation to the pyrolytic experiments due to the following common methodological features: (1) the objects under the study are volatilized; (2) the temperature conditions are very harsh; (3) the major products are PDs.

Despite the high PD yields, it seems quite reasonable to expect some thermal decomposition processes when amino acids are subjected to the temperatures above 200°C. We observed that in some cases the crude products have more or less intense yellow coloration, i.e., the PDs formed have impurities. Their chemical nature was unclear but evidently less polar than that of PDs, since the impurities were found to be dissolved easily in non-polar solvents, e.g., chloroform. Another observation, namely an increase in the amount of impurities at higher sublimation temperatures, pointed to the fact that they form as a result of decomposition processes. Finally, these impurities could not result from amino acid destruction through commonly known decarboxylation and deamination, since the latter produces volatile compounds like amines and carboxylic acids which would not condense under reduced pressure along with the PDs synthesized.

We found the above observations of certain theoretical and practical interest. In order to elucidate chemical structure of the impurities, in the present study we reproduced the sublimation of L-alanine (Ala), α-methylalanine (or α-aminoisobutyric acid, Aib), L-valine (Val) and L-leucine (Leu) in the presence of silica gel at higher temperatures, 230–250°C. After separating the impurities from PDs, their composition was studied by means of HPLC–particle beam (PB)-MS and GC–FTIR–MS. In order to facilitate assignment of the FTIR data, we also performed auxiliary computer simulation of IR spectra.

2. Experimental

2.1. Chemicals

Commercially available amino acids Aib, L-Ala, L-Val and L-Leu from Sigma (St. Louis, MO, USA; 99% purity), silica gel (from Aldrich, Milwaukee, WI, USA) and solvents were used without further purification.

2.2. Sample preparation

The typical sublimation procedure consisted of heating the mixture of crystalline amino acid (4 g) and silica gel (10 g) in a continuously evacuated round-bottom flask at about 10^{-1} Torr under 230–

250°C (1 Torr = 133.322 Pa). During the heating process, the amino acid sublimed, reacted with silica surface, and the resulting products along with unreacted amino acid condensed in the unheated flask neck. To convert more starting reagent to the products, the condensed sublimate was returned to the bottom containing silica gel, and the procedure was repeated under the same conditions two more times. Such triple sublimation took, in total, 7–9 h. Crude sublimates were removed from the flask neck and washed with chloroform to separate less-polar products from unreacted amino acids and PDs (major condensation products). The resulting solutions were evaporated to dryness giving yellow to brown amorphous substances (chloroform extracts, CHEs). The amounts of PDs and CHEs isolated are specified in Table 1.

2.3. Apparatus

For HPLC–PB-MS measurements, a Hewlett-Packard 1090 Series II liquid chromatograph was coupled with an HP 5989 mass spectrometer through an HP 59980B particle beam LC–MS interface. A column, 100×2.1 mm I.D. packed with 5 μm ODS Hypersil was used. Water–methanol was used as a mobile phase, with the uniform gradient program from 0% methanol to 20% at 30 min (for Aib and Ala) or to 100% methanol at 40 min (for Val and Leu); flow-rate, 1 ml min^{-1}; temperature, 45°C. Auxiliary UV detection at 200 nm was used to monitor the content of unreacted amino acids in the sublimates. The temperature of the PB nebulizer was 60°C.

For GC–FTIR–MS analyses, a HP 5890 Series II Plus gas chromatograph was coupled in parallel with a HP 5965B FTIR detector and a HP 5989 mass spectrometer. The GC column was a HP-5 (cross-linked 5% phenyl-methyl silicone), 25 m×0.32 mm I.D., film thickness 0.52 μm, phase ratio 150. Injection, 250°C. Carrier gas: He at 2 ml min^{-1}. Oven programs: (A) 50°C (10 min) to 130°C at 10°C min^{-1}, to 240°C at 2.5°C min^{-1}; (B) 50°C to 250°C at 10°C min^{-1}. The IR cell and interfaces were kept at 250°C. The FTIR data were acquired at the resolution of 4 cm^{-1}. The ionization energy was 70 eV both for GC–FTIR–MS and for HPLC–PB-MS measurements.

Table 1
Yields (in g and %) of piperazinediones (PDs) and chloroform extracts (CHEs) resulting from the sublimation of amino acids in the presence of silica gel at 230–250°C

Starting amino acid	PD		CHE (g)
	(g)	(%)	
Aib	1.35	41	0.27
L-Ala	1.50	47	1.27
L-Val	2.03	59	0.25
L-Leu	1.21	35	1.18

2.4. Computer simulations

For IR spectra simulations, the program HyperChem (from Hypercube, Canada) was used. Before the calculations, energy minimization was performed by the PM3 semi-empirical method (convergence limit of 0.008 kcal mol^{-1}; 1 cal = 4.184 J). For IR simulations the same method was utilized. All the calculations refer to isolated molecules in vacuo.

3. Results and discussion

3.1. Yields of the products

Under the temperature of 230–250°C and reduced pressure, silica gel catalyzes nearly quantitative condensation of the amino acids, with PDs being the major products in yields of 35–59% (Table 1). Only traces of the starting amino acids can be detected by means of HPLC. At the same time, along with PDs, less-polar compounds form and can be separated by chloroform extraction. Their amounts (Table 1; CHEs) were found to be of the same order of magnitude as those for PDs.

3.2. HPLC–PB-MS measurements

At the first stage, we analyzed CHEs using HPLC–PB-MS. Due to relatively low temperatures in the chromatographic system (45°C) and PB nebulizer (60°C), the compounds studied were safe from any thermal decomposition processes up to the ionization source chamber. Fig. 1 shows typical examples of the resulting chromatograms. Analyzing

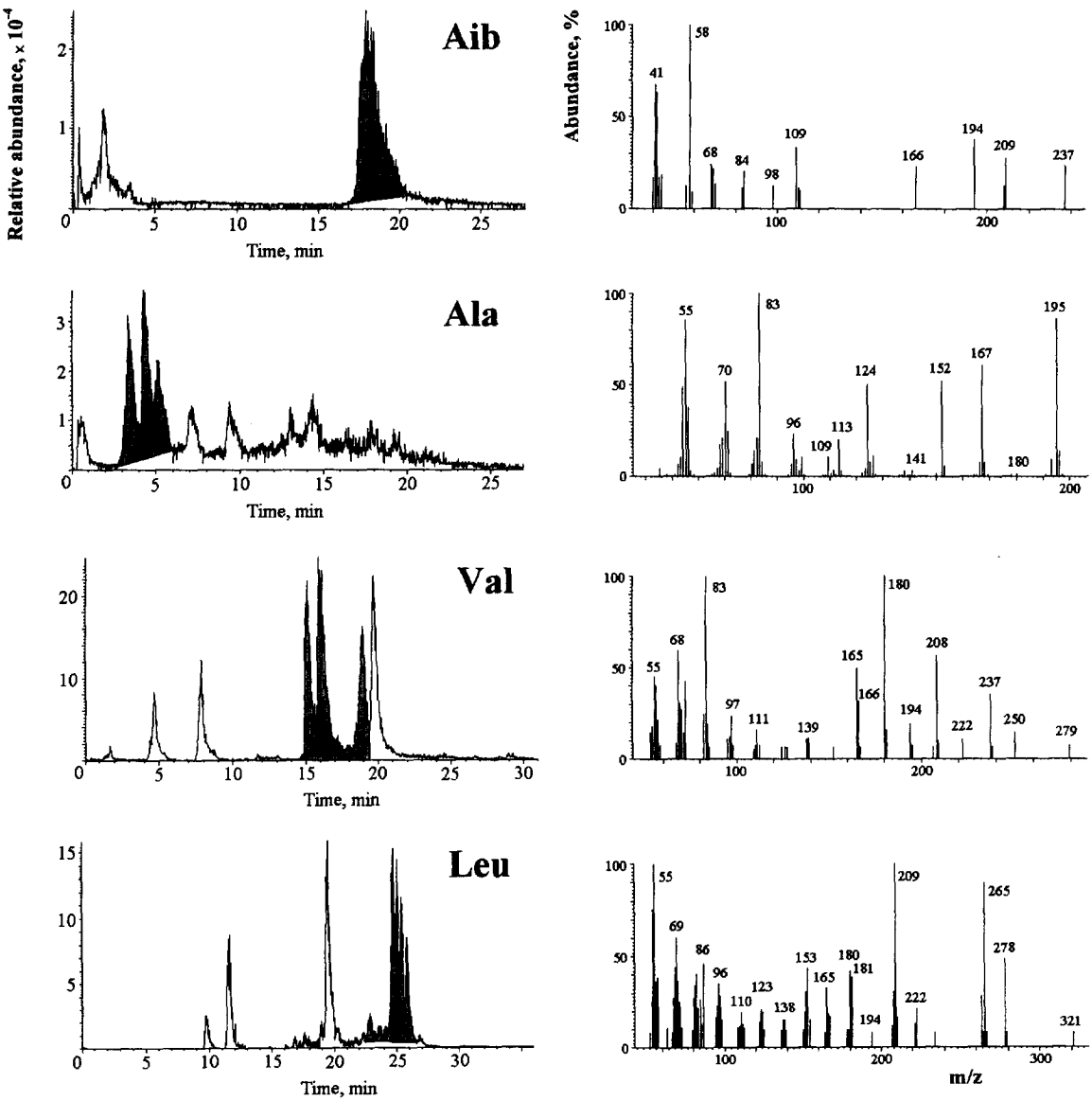

Fig. 1. HPLC–PB-MS total ion chromatograms (left) of CHEs extracted from Aib, Ala, Val and Leu sublimates, and 70 eV electron impact mass spectra (right) for the peaks highlighted in the chromatograms.

electron impact (EI) mass spectra for the major chromatographic peaks we found that some of the compounds (peaks highlighted in Fig. 1, left) have molecular ions obeying the following rule: the products are composed of three amino acid molecules which have lost four water molecules, e.g., at *m/z* 237 for Aib, 195 for Ala, 279 for Val and 321 for Leu (Fig. 1, right). For Aib (an optically inactive amino acid) only one chromatographic peak is observed, whereas in the other cases at least three peaks are clearly distinguished, having the same fragmentation pattern. This can be attributed to the formation of diastereomeric compounds, and thus one can conclude that significant racemization occurs

during the sublimation experiments. The EI patterns (Fig. 1, right) have many common features with those characteristic for PDs [9,14]. The most important are the series of peaks corresponding to a (random order) stepwise loss of CO (*m/z* 28) and HNCO (*m/z* 43) moieties during fragmentation: e.g., at *m/z* 237-209-166 and 237-194-166 for Aib, 195-167-124 and 195-152-124 for Ala, 237-194-166 for Val, 265-222-194 and 209-181-138 for Leu. Whether the losses of CO and HNCO occur from the molecular ion or from a fragment ion such as that for valine at *m/z* 237 (which probably represents an ion resulting from the loss of propene from the molecular ion), these losses indicate the presence of at least two amide (or peptide) bonds in the compounds analyzed, similar to the case of PDs.

To explain the possible structure of the compounds detected, we considered the possibility of one of the two NH groups in a PD molecule, already forming a peptide bond, to be additionally acylated by a third amino acid molecule giving the following imide:

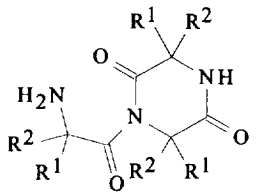

$R^1=R^2=CH_3$ (Aib); $R^1=H$; $R^2=CH_3$ (Ala), $CH(CH_3)_2$ (Val), $CH_2CH(CH_3)_2$ (Leu)

Then, there is a possibility of losing one more water molecule forming bicyclic amidine (BCA)

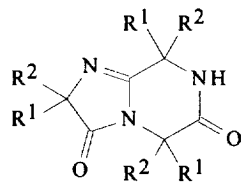

BCA

One known example of BCA has been described for the case of Aib [15–17]. The compound has been synthesized by cyclizing tri-, tetra- or penta-Aib peptide derivatives, whereas its formation directly from the amino acid was not described.

Other peaks in the chromatograms in Fig. 1 had molecular ions in the corresponding EI mass spectra at lower *m/z* than the highlighted peaks had. The mass spectra themselves were not in all cases of such good quality as those presented in Fig. 1 (right) and did not allow compound identification. For this reason we focused on analyses of the samples by means of the GC–FTIR–MS technique.

3.3. GC–FTIR–MS measurements

Of the peaks detected in the Aib CHE chromatogram (Fig. 2) a good quality FTIR and EI mass spectra have been afforded only for the four numbered components. These spectral data are presented in Fig. 3. The peak 3 (compound **Aib-3**) has been found to have the same molecular ion (*m/z* 237) and generally the same fragmentation pattern as the highlighted peak in the HPLC–PB-MS chromatogram (Fig. 1). Its FTIR spectrum exhibits three sharp bands in the region of 1600–1800 cm^{-1}, which can be attributed to stretching vibrations of C=O (two types) and C=N bonds in the BCA molecule. Accepting this assumed structure, we performed computer simulation of its IR spectrum, which is presented in Fig. 3. Similarity to the experimental FTIR spectrum is obvious: the calculated spectrum presents the same three sharp bands due to the double bonds ($\nu_{C=X}$, where X=C, N, O). The shift to higher wavenumbers by about 10% is common for the semi-empirical method PM3 [18]. All these data unambiguously prove the bicyclic amidine structure for the compound **Aib-3**.

The compounds **Aib-1** and **Aib-2** (peaks 1 and 2 in Fig. 2) have lower molecular masses than the previous CHE component (*m/z* 179 and 125, respec-

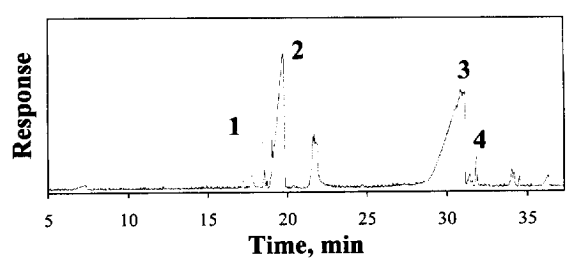

Fig. 2. GC–FTIR total response chromatogram of Aib CHE. Oven program A.

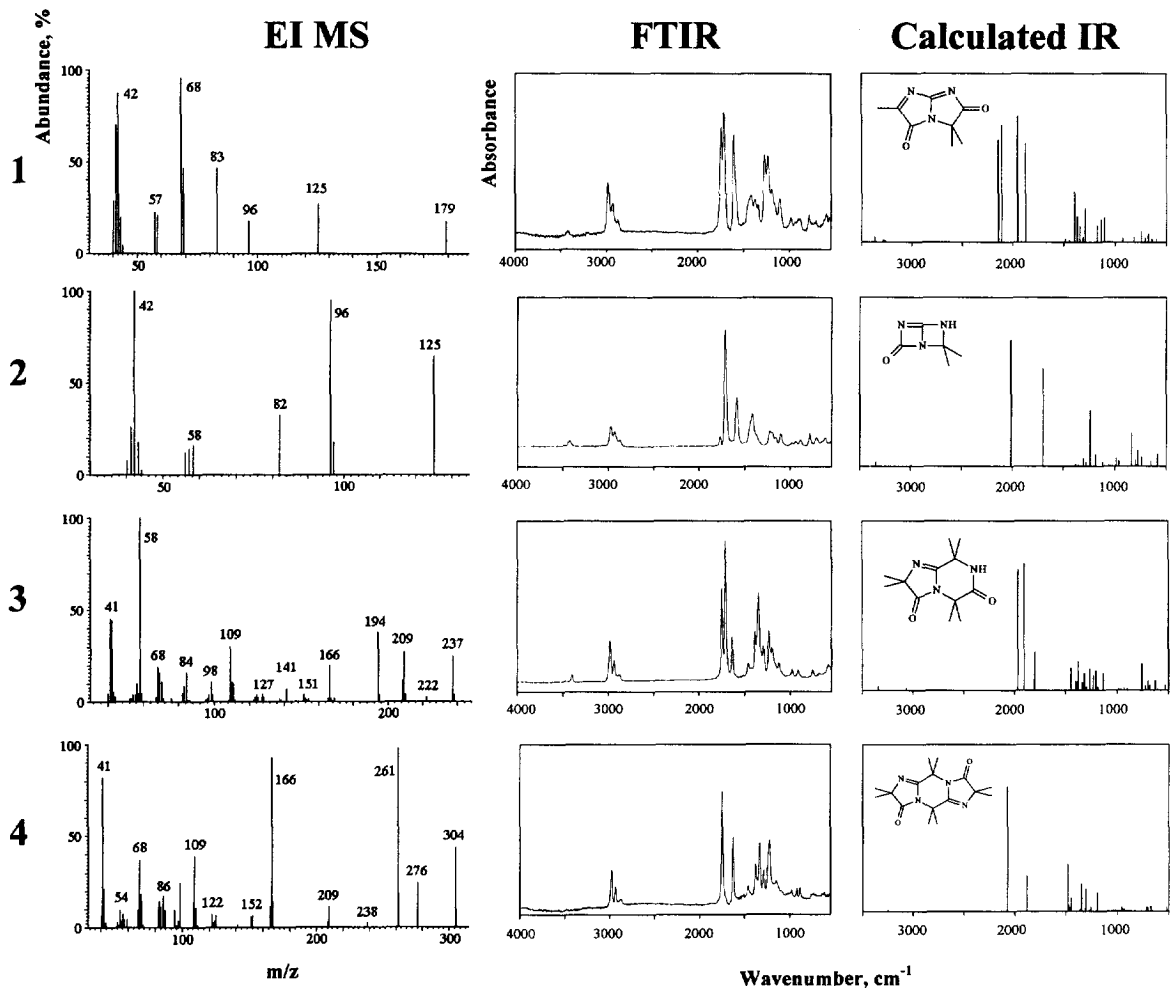

Fig. 3. Identification of the Aib CHE components (**Aib-1** to **Aib-4**) based on the experimental EI-MS, FTIR and calculated IR spectra.

tively), pointing to the fact that they might be degradation or decomposition products. **Aib-1** can be tentatively identified as the amidine **Aib-3** minus CH_4 and $C(CH_3)_2$; and **Aib-2**, as the amidine **Aib-3** minus $2C(CH_3)_2$ and CO. However exact sites of the ring cleavage cannot be easily determined. We attempted to find them varying possible molecular structures and simulating IR spectra, but no theoretical spectra obtained exactly matched the experimental ones. Those presented in Fig. 3 best correspond to the experimental FTIR spectra.

EI mass spectrum of the last component **Aib-4** contains a peak due to molecular ion at *m/z* 304. Such a molecular mass could have a compound composed of four amino acid molecules with the loss of six water molecules. The formation of a cyclic Aib tetrapeptide would be accompanied with the loss of four water molecules only. Instead, one can suggest that acylation of the NH group in BCA with subsequent cyclization, by analogy to the case of PD N-acylation/cyclization, leads to tricyclic amidine (TCA):

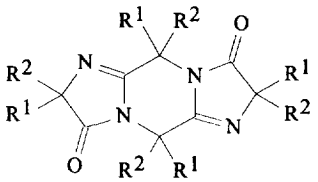

TCA

The only known example of TCA has been described, along with the related BCA, for the case of Aib [16,17]: it has been synthesized by cyclizing tetra- or penta-Aib peptide chlorides, whereas formation directly from the amino acid has not been documented.

The experimental EI-MS and FTIR data confirm this supposition. Besides the peak of molecular ion (*m/z* 304) in the mass spectrum, there are peaks at *m/z* 276 and 261 which can be attributed to a stepwise loss of CO and $CH_3\cdot$ from Aib TCA molecule. Also important are peaks at *m/z* 166 and 152 due to the following fragments:

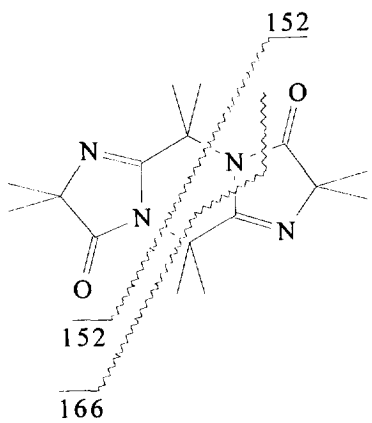

The FTIR spectrum presents only two bands in the region of 1600–1800 cm^{-1}, corresponding to one kind of C=O and one kind of C=N bonds (stretching vibrations), as it should be in the TCA. A similar IR spectrum has been obtained by means of the PM3 simulation. Thus, the compound **Aib-4** can be identified as Aib TCA.

A little more detailed spectral data, for six components, have been acquired for the case of Ala CHE (Fig. 5). The component **Ala-2** (triple peak 2 in Fig. 4) has essentially the same EI fragmentation pattern as measured by HPLC–PB-MS (Fig. 1) and, at the same time, a FTIR spectrum very similar to that of **Aib-3** (Fig. 3). Based on the above and on the data of computer IR spectrum simulation, this compound can be concluded to be the bicyclic amidine derivative of Ala.

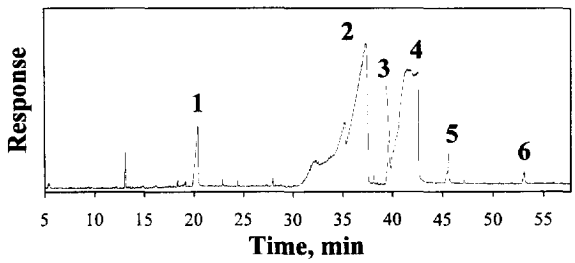

Fig. 4. GC–FTIR total response chromatogram of Ala CHE. Oven program A.

From the view point of assignment procedure, an interesting example is the compound **Ala-4**. Its molecular mass (*m/z* 193) is lower than the bicyclic amidine by 2. The mass spectrum contains a series of peaks at *m/z* 165-137-122 corresponding to a stepwise loss of 2CO and $CH_3\cdot$ groups from the molecular ion. The peak at *m/z* 150 is due to elimination of HNCO. In other words, such pattern evidences the existence in **Ala-4** molecules of the same structural fragments as those presented in BCA. In addition, the difference in the molecular masses of 2 points to the presence of one more double bond in **Ala-4**. Analysis of possible dehydrogenation sites provides five different possibilities. We performed the computer simulation of IR spectra for all of them. The results for the first four possible dehydrogenation products, which can be formed by simple hydrogen elimination from one of the CH_3 groups or from the piperazine ring, are shown in Fig. 6. Their unsimilarity to the experimental spectrum is evident. In the fifth option, we admitted hydrogen elimination to be accompanied by the C=N bond migration in the imidazole ring, and found that the resulting structure (Fig. 5) best reflects features of the experimental FTIR spectrum. Actually the calculated spectrum exhibits two bands due to stretching

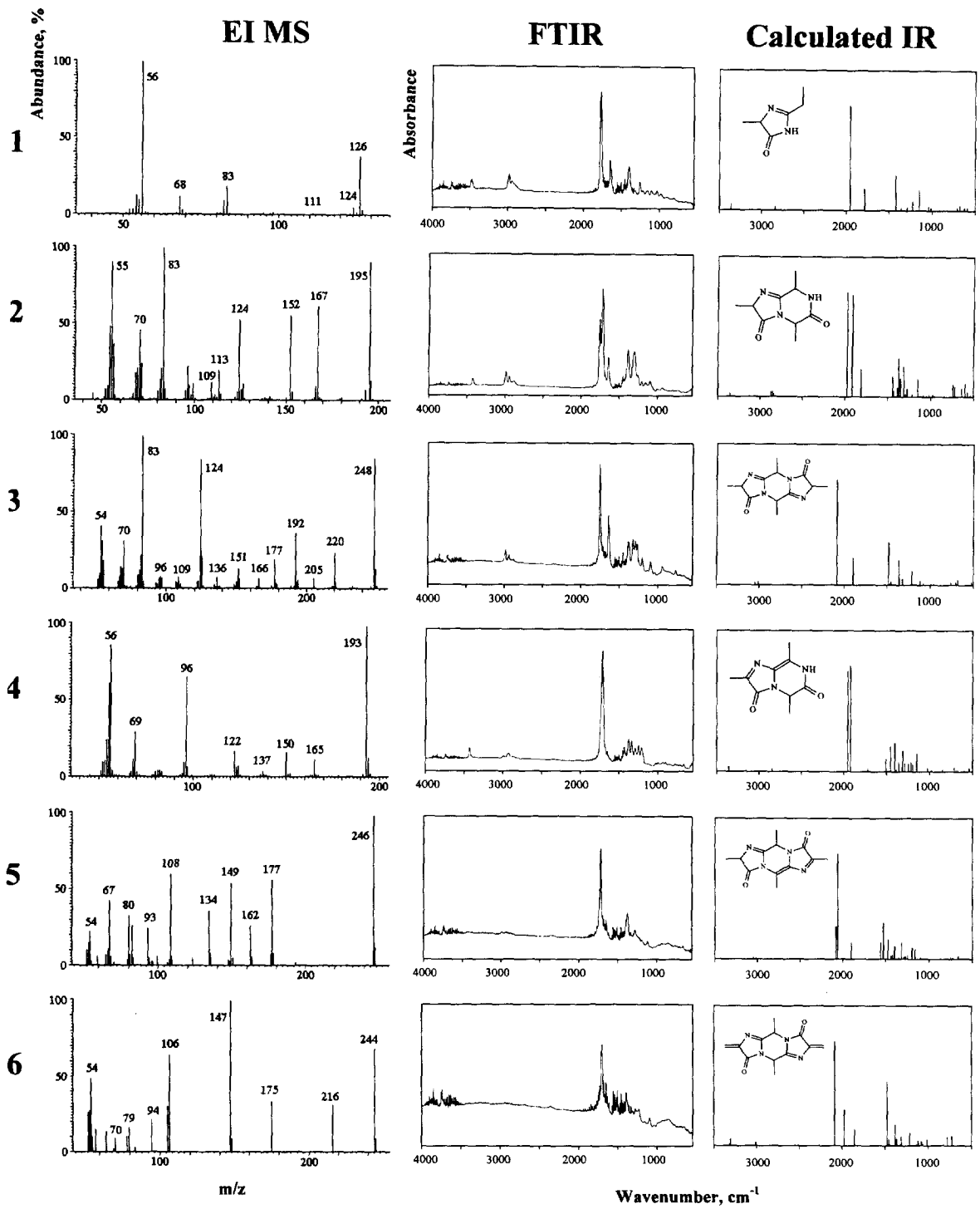

Fig. 5. Identification of the Ala CHE components (**Ala-1** to **Ala-6**) based on the experimental EI-MS, FTIR and calculated IR spectra.

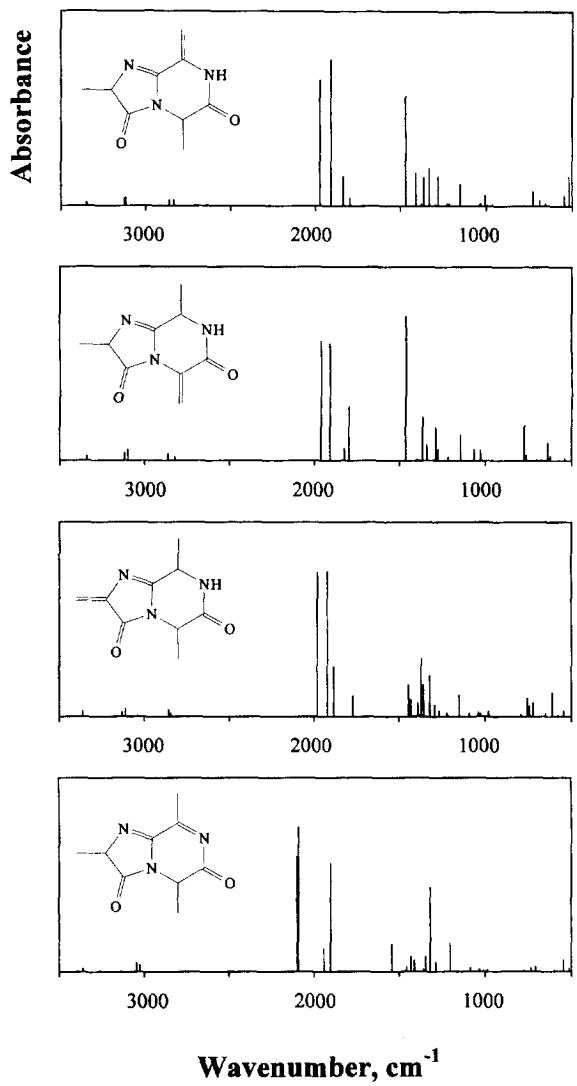

Fig. 6. Comparison of calculated IR spectra for the dehydrated isomeric amidines alternative to the structure **Ala-4** (Fig. 5).

vibrations of double bonds, contrary to the single band in the experimental one. Nevertheless, closer consideration reveals that the width of the latter is noticeably bigger than for other compounds' absorption bands in this region, so that it can be two overlapping bands which cannot be resolved with the FTIR detector used.

Chromatographic peaks 3, 5 and 6 (Fig. 4) were even more interesting. The first component, **Ala-3**, having molecular ion at m/z 248 and FTIR spectrum with two adsorption bands in the region of 1600–1800 cm^{-1}, has been identified as TCA. It has almost the same spectral features (both in the experimental and calculated spectra) as its analog **Aib-4**. Similarly to the latter, the EI fragmentation patterns includes the peak corresponding to the cleavage

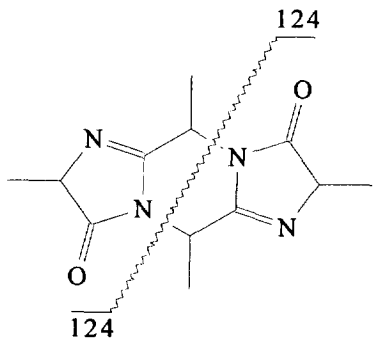

(m/z 124). Just this site of cleavage and not, for example, the following one

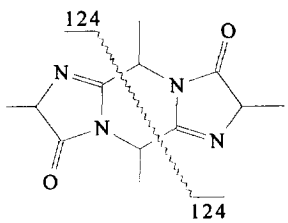

is confirmed by the revealing **Ala-1** compound, having HNCO group (to its loss during fragmentation corresponds the peak at m/z 83). On the contrary, the second way of pyrolytic cleavage of both TCA and BCA would produce the imidazole derivative which does not have NH moiety:

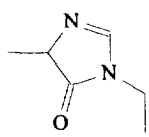

According to the peaks of molecular ions at m/z 246 and 244, the components **Ala-5** and **Ala-6** are dehydrogenated and doubly dehydrogenated TCA, respectively. These cases are even more complicated than the dehydrogenated BCA, since the existence of four methyl groups provides more possible sites of dehydrogenation resulting in higher number of possible isomers. After analysis of all the options and

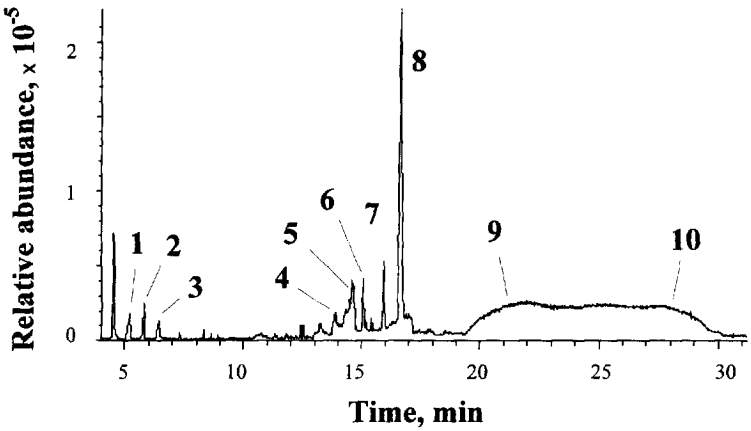

Fig. 7. GC–MS total ion chromatogram of Val CHE. Oven program B.

their IR spectra simulations, we assigned to peaks 5 and 6 (Fig. 4) the structures presented in Fig. 5.

The chromatogram of Val CHE (Fig. 7) has a bright distinctive feature as compared to the previous two cases. Between 19 and 30 min, a very broad diffuse peak is observed, apparently corresponding to a compound decomposing slowly in the GC column. It was possible to analyze EI-MS and FTIR spectra of the eluent at different times during this broad diffuse peak. As a result, gradual spectral changes have been found within the whole peak. In the peak's beginning, the FTIR spectrum (Fig. 8) has the same three double-bond bands characteristic for the BCAs **Aib-3** and **Ala-2** as well as a very similar general view. However, the molecular ion has been found to be at *m/z* 237 and not at 279, as it should be for the corresponding BCA and as it was really found during HPLC–PB-MS measurements (Fig. 1). We attribute this disagreement to slow thermal decomposition of Val BCA in the chromatographic column (at this point the gradient temperature is 250°C) with the loss of one of three isopropyl substituents as propene molecule (*m/z* 42). Such thermal decomposition pattern was already described for the case of Val PDs by Smith et al. [9]. The resulting molecule is, as a matter of fact, also a BCA derived from two Val residues and one Gly residue with uncertain (from the experimental FTIR and calculated IR spectra) amino acid sequence, for instance as presented in Fig. 8 (**Val-9**). The EI-MS suggests just this proposed structure due to the fragmentation

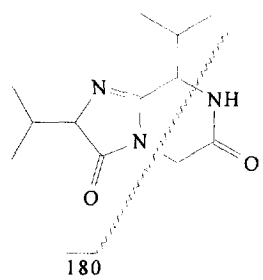

Other important peaks are the series at *m/z* 194-166-138 due to a stepwise loss of $C_3H_7\cdot$ and two CO groups.

At 25–30 min (Fig. 7) another decomposition product prevails. It was rather easy to assign it as a dehydrogenated BCA, since the EI mass spectrum contains a very intense molecular ion peak at *m/z* 277 (Fig. 8). In addition, obvious similarity between the FTIR spectra of this compound and that of **Ala-4** indicates dehydrogenation with double bond rearrangement. Again, as in the latter case, the IR spectrum simulation for the most probable structure **Val-10** gave two close peaks instead of one peak recorded experimentally.

The detection of one more CHE component (**Val-7**) possessing very similar spectral properties, especially the same molecular mass of 277 (Fig. 8) was rather unexpected. Moreover, its FTIR spectrum,

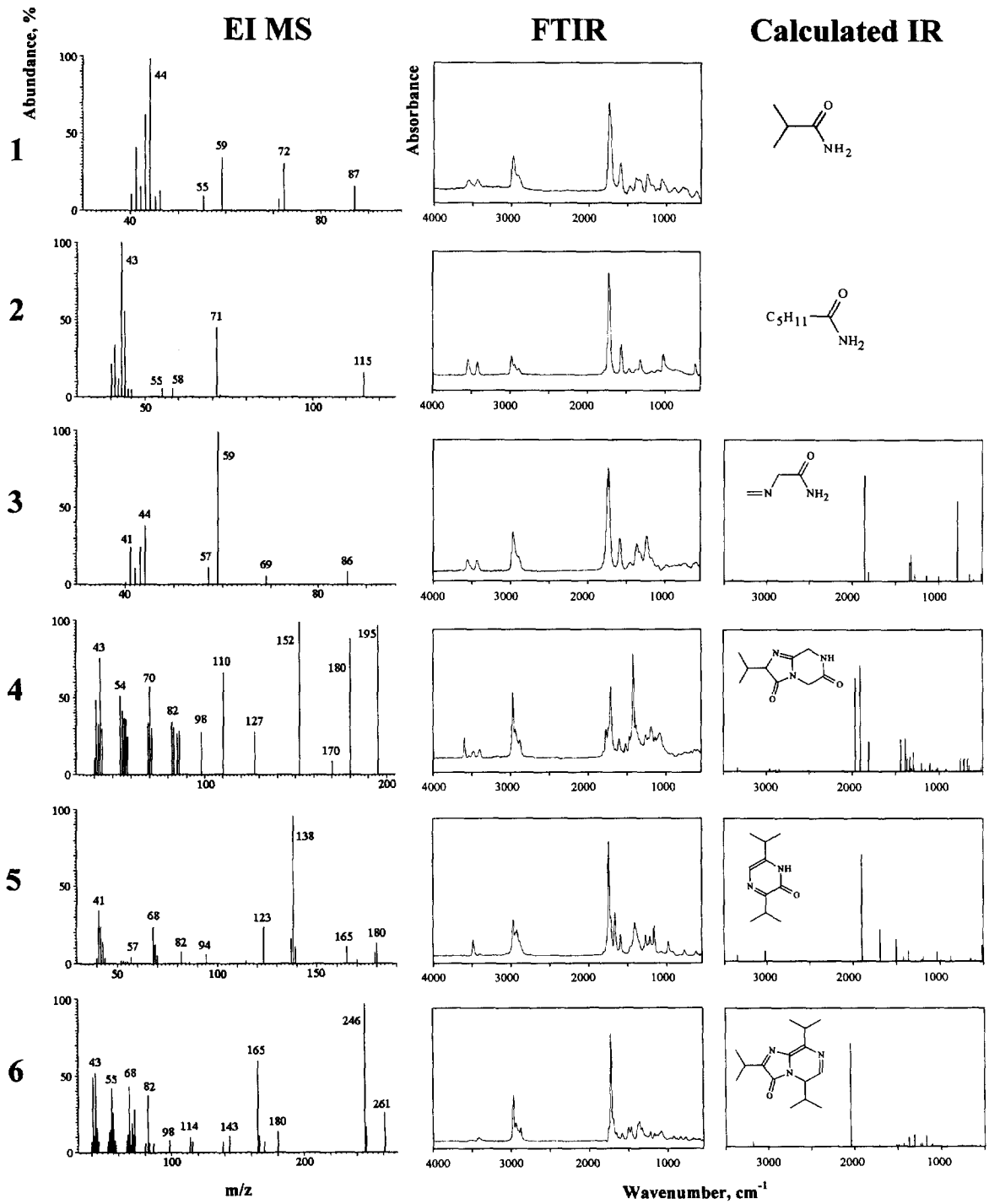

Fig. 8. Identification of the Val CHE components (**Val-1** to **Val-10**) based on the experimental EI-MS, FTIR and calculated IR spectra.

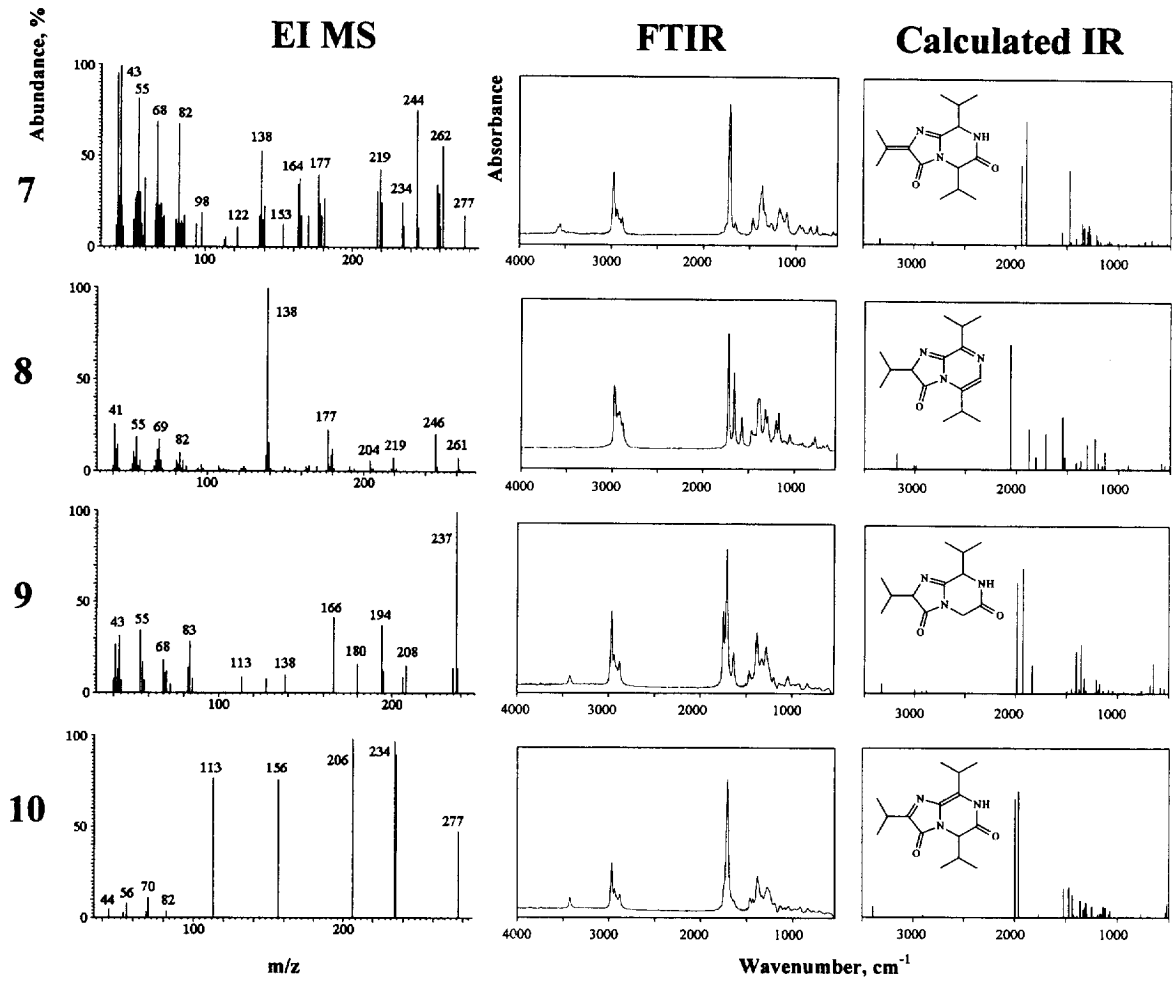

Fig. 8. (*continued*)

having a sharp $\nu_{C=O}$ band at about 1700 cm^{-1}, also appears very similar to that of **Val-10**. A noticeable difference, however, is the shift of ν_{NH} band to about 3600 cm^{-1} as compared to about 3450 cm^{-1} recorded for the latter. This shift suggests the absence of a double C=C bond in the position neighbouring to the NH group in **Val-7**. According to the results of IR spectra simulations, the most likely site of dehydrogenation is the methyne groups of the imidazole ring (structure shown in Fig. 8). During the electron impact ionization the **Val-7** molecule first loses one of the methyl groups (*m/z* 262); then either a stepwise cleavage of $C_3H_7\cdot$ (or HNCO; *m/z* 219) and C_3H_6 (*m/z* 177)/$C_4H_7\cdot$ (*m/z* 164) or the loss of H_2O (*m/z* 244) is observed.

Interestingly, dehydration is one of the major pathways for Val BCA thermal decomposition. It produces significant amount of the component **Val-8** and smaller amount of **Val-6** (Fig. 7), both having a molecular mass of 261 (Fig. 8). Contrary to the previous three Val derivatives, their FTIR spectra do not have a sharp ν_{NH} band in the region of 3400–3600 cm^{-1} (the diffuse absorption is still expressed for **Val-6**, probably to some tautomeric equilibrium). Supposing that dehydration affects the piperazine ring, we performed IR spectra simulations and found

two preferable structures (Fig. 8). For **Val-6**, only one absorption band due to stretching vibrations of the double bonds has been afforded, confirming the experimental FTIR spectrum: this single band is due to the formation of totally conjugated system beginning with the C=O group of the imidazolone moiety. In the **Val-8** molecule, the latter group is separated from other double bonds resulting in three sharp $\nu_{C=X}$ bands in the FTIR spectrum; in the calculated spectrum, all four bands can be distinguished.

The least of Val CHE components detected is the component **Val-4**. It produces a small chromatographic peak (Fig. 7) and has a molecular mass of 195, according to the EI mass spectrum (Fig. 8). We were unable to obtain a good-quality FTIR spectrum for this compound, and that presented in Fig. 8 evidently reflects its contamination with some other component: besides the single ν_{NH} band at about 3600 cm^{-1} due to the ring NH group, other two ν_{NH} bands are clearly seen at about 3400 and 3500 cm^{-1} which are due to ν_{NH} (asymmetric) and ν_{NH} (symmetric) vibrations, respectively, of NH_2 groups of an unidentified amine or amide. In the low frequency region the picture is even more complicated due to overlapping bands, and based on this spectrum exact identification of **Val-4** is impossible, even using the computer simulation. However, accounting for presence of the dealkylated BCA **Val-9** in the chloroform extract, and for a principal possibility for the latter component to lose one more alkyl substituent as C_3H_6 molecule giving a compound with the molecular mass of 195, we have tentatively assigned to **Val-4** the structure shown in Fig. 8.

From the remaining four CHE components (Fig. 7) the most abundant, according to the chromatogram, was the compound **Val-5**. Its molecular mass has been found to be 180 (Fig. 8), that might correspond to a dehydrated Val PD (Val PDs molecular mass is 198). The fragmentation pattern including the pairs of peaks at *m/z* 138-94 and 138-82 due to the losses $-C_3H_6$-C_3H_8 and $-C_3H_6$-C_4H_8, respectively, suggests two isopropyl α-substituents to be present in the molecule of **Val-5**. The FTIR spectrum exhibits three $\nu_{C=X}$ bands in the region of 1600–1800 cm^{-1} and one ν_{NH} band at about 3500 cm^{-1}. We performed IR spectra calculations for two isomeric dehydrated PDs possible; the IR spectrum presented in Fig. 8 best matches the experimental one.

The components **Val-1**, **Val-2** and **Val-3** have in their FTIR spectra all the features characteristic for primary amides: (1) two ν_{NH} bands at about 3450 and 3550 cm^{-1} due to ν_{NH}(asymmetric) and ν_{NH}(symmetric) vibrations of NH_2 groups; (2) $\nu_{C=O}$ band ("amide I") at 1700–1750 cm^{-1}; (3) δ_{NH} band ("amide II") at 1550–1600 cm^{-1}, approximately three times less intense than the "amide I" band (Fig. 8). Computer simulation of IR spectra for such class of compounds (other primary amides were also tested) gave unsatisfactory results; in particular, the simulated spectra did not exhibit realistic vibration modes (both ν_{NH} and δ_{NH}) for NH groups, as it is exemplified by the case of **Val-3** (Fig. 8). So we can provide their tentative identification based on the comparison of the FTIR spectra measured with those available in the literature [19] and on the EI mass spectra. In the latter, two ions are present typical for primary amides:

m/z 44 m/z 59

A particular feature for **Val-2** (molecular mass of 115) is the series of fragments at *m/z* 43-55-71 due to hydrocarbon ions $C_3H_7^+$, $C_4H_7^+$ and $C_5H_{11}^+$ suggesting the presence of a C_5H_{11} substituent of uncertain spatial configuration.

Unlike the cases of Aib and Ala CHEs, no traces of Val tricyclic derivatives or their evident decomposition products have been detected.

The same result has been obtained for the case of Leu. The chromatogram's general view is similar to that of Val CHE. Especially it regards to a very broad peak ranging from 22 to 42 min (Fig. 9), due to thermal decomposition of a major (according to the peak area) component. We analyzed EI-MS and FTIR spectra in its different places, and, as in the case of Val CHE, found gradual spectral changes within the whole peak. Initially (e.g., at 26 min; **Leu-9**) the FTIR (Fig. 10) has the same three $\nu_{C=X}$ bands typical for the BCAs **Aib-3** and **Ala-2** as well as for the dealkylated BCA **Val-9**. The EI-MS

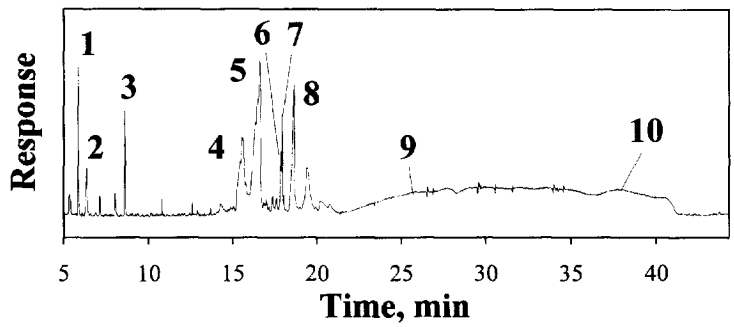

Fig. 9. GC–FTIR total response chromatogram of Leu CHE. Oven program B.

analysis shows the presence of a molecular ion peak at m/z 265, which might correspond to a dealkylated ($-C_4H_8$) Leu BCA analogous to **Val-9**. In addition, other peaks can be identified corresponding to the loss of a second isobutyl substituent as C_4H_8 (m/z 209), to hydrocarbon ions $C_3H_6\cdot^+$ (m/z 42), $C_4H_7^+$ (m/z 55) and to the fragment $C_4H_9CH{=}NH_2^+$ (m/z 86) fromed according to the mechanism shown in Fig. 11. The last ion can serve as a strong evidence for the formation of **Leu-9** as a result of C(5) dealkylation. The calculated IR spectrum is in a good accordance with this proposed structure.

In the later part of the diffuse peak (Fig. 9) the compound **Leu-10** prevails having a molecular mass of 263 (Fig. 10), i.e., differing from **Leu-9** by 2. The EI mass spectrum was not of a good quality, and besides the molecular ion (the most abundant), only two hydrocarbon ions $C_3H_5^+$ (m/z 41) and $C_4H_7^+$ (m/z 55) have been detected. One can suggest this compound to be Leu BCA dealkylated due to the cleavage of isobutane C_4H_{10}, and not of isobutene as in the case of **Leu-9**. The experimental FTIR spectrum has, however, a small but important feature as compared to the spectra of analogous dehydrogenated products **Ala-4** (Fig. 5) and **Val-10** (Fig. 8): differentiation of the composite $\nu_{C=X}$ band at about 1700 cm^{-1} to two overlapping bands is clearly seen, as appeared in the calculated IR spectra of **Ala-4** and **Val-10**, and was obtained again for the proposed structure of **Leu-10** (Fig. 10). This difference from the Ala and Val derivatives is apparently due to a relatively big size of the isobutyl substituents resulting in some distortion of the bicyclic ring system.

The components **Leu-7** and **Leu-8** have the same molecular mass of 303 and a number of peaks due to the cleavage of hydrocarbon moieties (Fig. 10). The molecular mass differs by 18 from the molecular mass of the Leu BCA (Fig. 1), thus strongly suggesting both compounds to result from the BCA dehydration. Their FTIR spectra do not coincide: for **Leu-7** only one $\nu_{C=X}$ band has been recorded, whereas **Leu-8** has three bands in the region of 1500–1800 cm^{-1} completely separated. Two isomeric dehydrated BCAs are possible, similarly to **Val-6** and **Val-8**, and the results of IR spectra simulations allowed us to identify them as the compounds **Leu-7** and **Leu-8** shown in Fig. 10.

In general, Leu BCA derivatives appear less stable thermally than other amino acids' BCAs studied, and all six remaining compounds identified (as well as many unidentified products of relatively low molecular masses) are the products of complete or partial destruction of the imidazo[1,2-*a*]pyrazine system. The component **Leu-6** has the highest molecular mass, 262 (Fig. 10). The FTIR spectral features are two $\nu_{C=X}$ bands and the absence of ν_{NH} band in the high-frequency range. From common considerations, accounting for the abundance of **Leu-9** and **Leu-10**, one may expect this compound to originate from them through the loss of side chains or some fragments of the cyclic system. As it has been shown by Smith et al. [9], one of the pathways observed for PD thermal destruction is cleavage of the amide bond as HNCO. Accepting that the related BCAs undergo the same reaction, we can propose that **Leu-6** is the product of HNCO elimination and the loss of a methyl group (as CH_4) from one of the alkyl side-chains. We performed analysis of all the

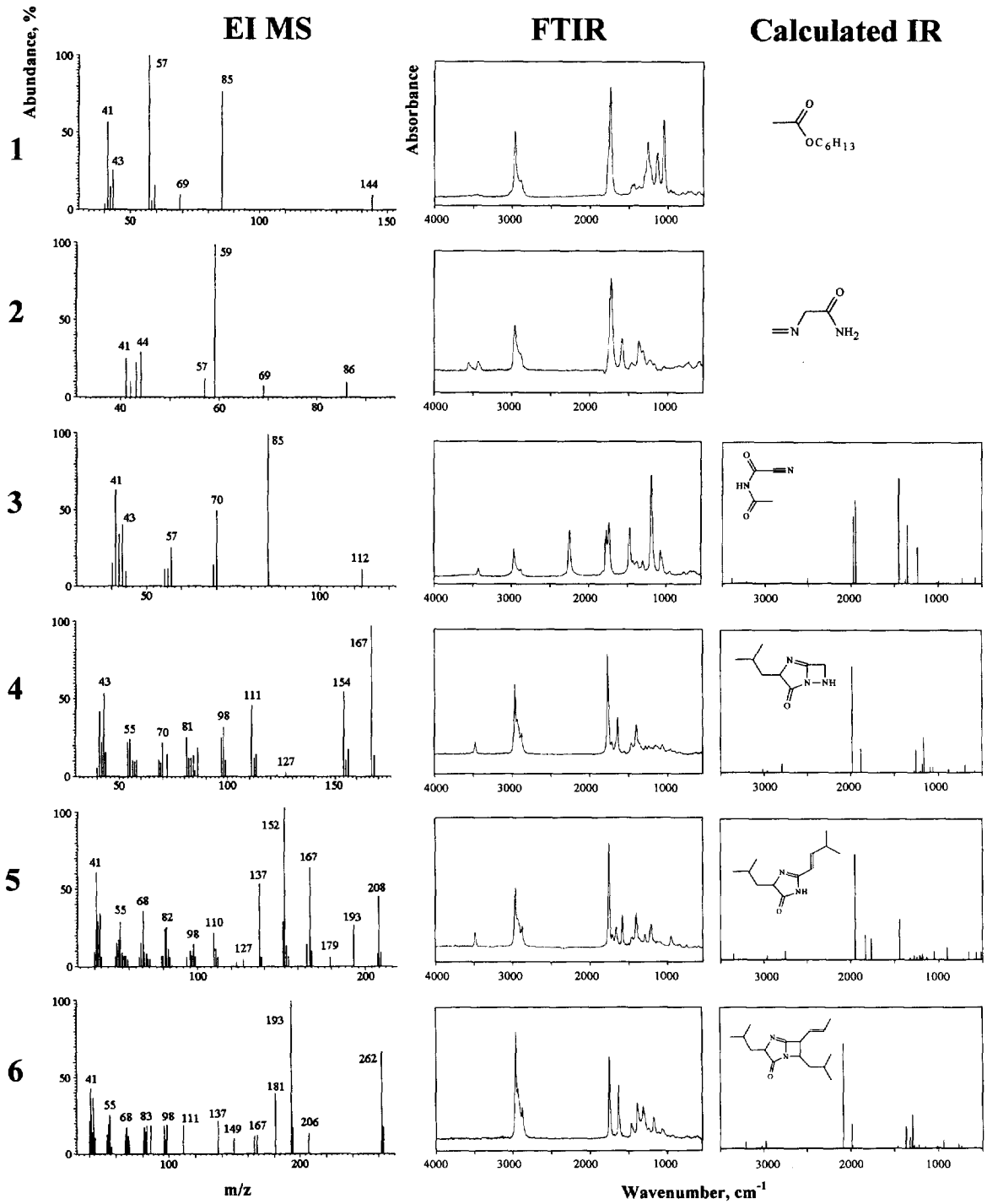

Fig. 10. Identification of the Leu CHE components (**Leu-1** to **Leu-10**) based on the experimental EI-MS, FTIR and calculated IR spectra.

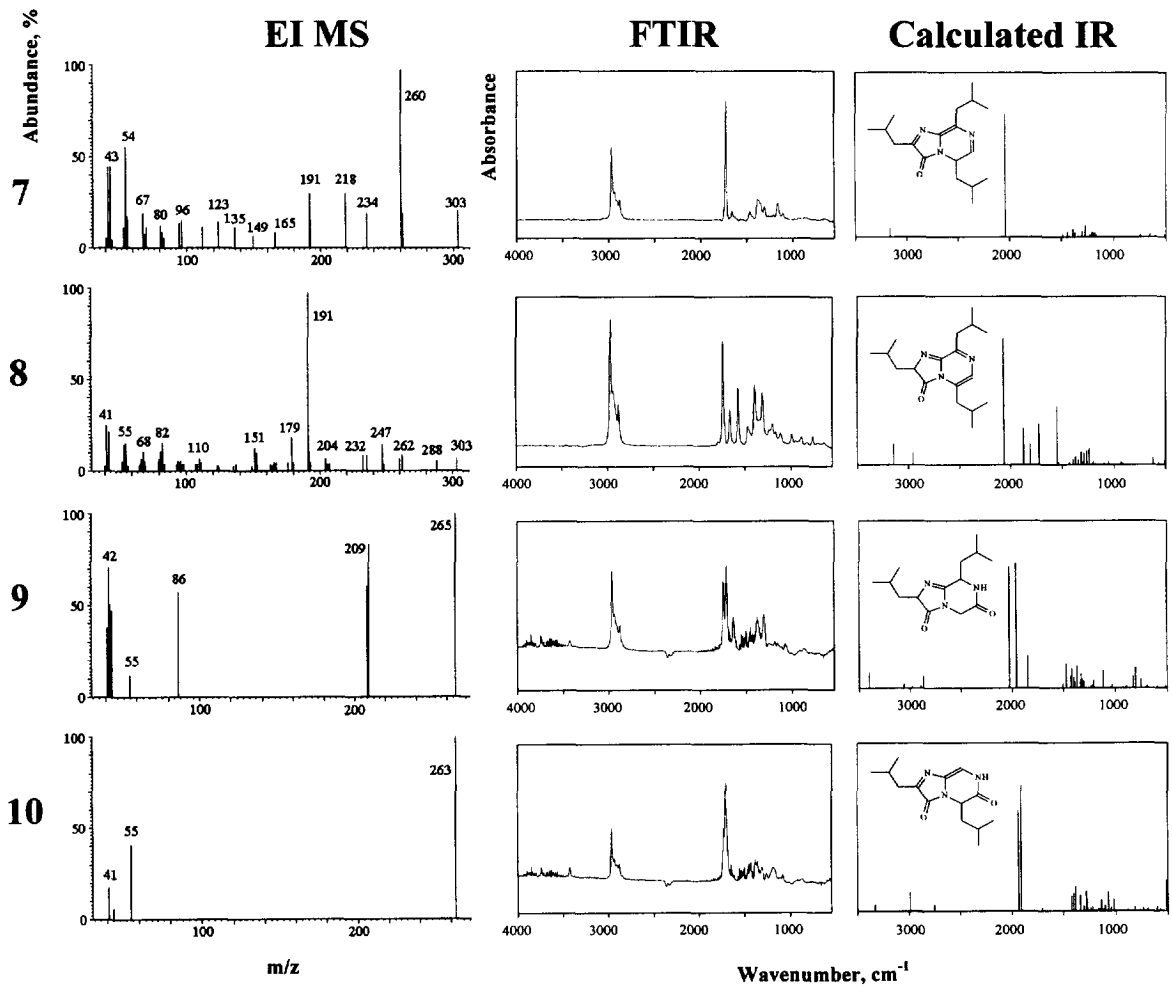

Fig. 10. (*continued*)

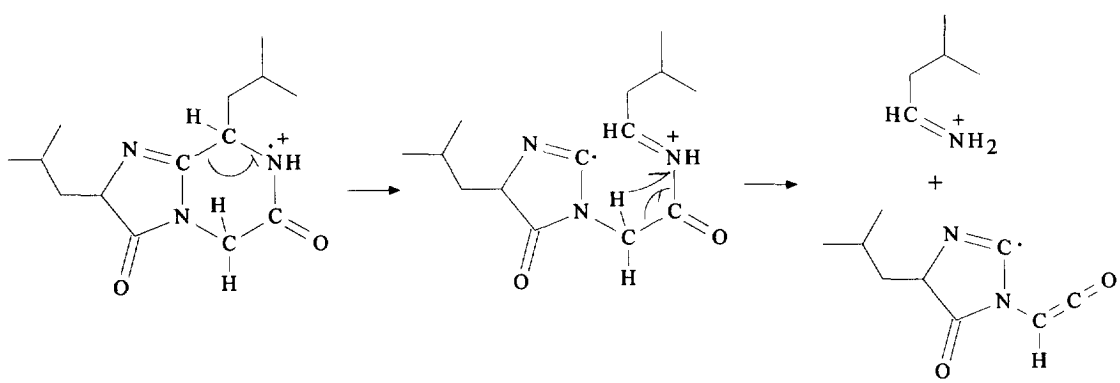

Fig. 11. Mechanism of **Leu-9** fragmentation producing the ion $C_4H_9CH{=}NH_2^+$.

possible choices and simulation of their IR spectra, and believe this compound to have the structure presented in Fig. 10. Its EI fragmentation pattern can be satisfactory explained as in Fig. 12 (the structural formulae are shown simply to exemplify possible sites of cleaving hydrocarbon moieties: the fragments with *m/z* 98, 137, 149, 181, 193 and 206 are inferred to have similar origin).

Apparently related decomposition process leads to the formation of **Leu-5**. According to the FTIR spectrum (Fig. 10), this compound has three double bonds (C=O, C=N and C=C) and one NH bond (medium-intensity sharp band at about 3600 cm^{-1}). The molecular mass is 208, and the EI fragmentation pattern is remnant of the spectrum of **Leu-6**. It includes the same ions at *m/z* 193, 167 and 137 as well as other ions which can be attributed to the loss of the alkyl substituents, for instance as C_4H_8 (*m/z* 152), as well as the pair of ions at *m/z* 98 and 110 due to the cleavage of the following accepted structure (confirmed by the simulation of IR spectra):

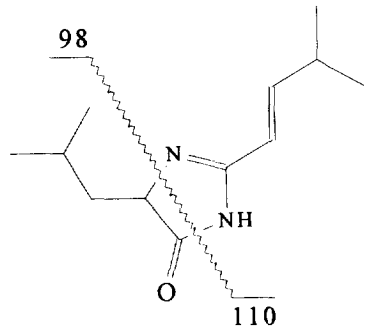

The component **Leu-4** has many similar spectral features, however at the same time only two C=X bonds. It corresponds to a higher degree of BCA thermal degradation with resulting molecular mass of 167 (Fig. 10). The last value evidences on the presence of three N-atoms in its molecule, contrary to two previous cases (**Leu-5** and **Leu-6**). Analysis of all the possible options with computer simulation of their IR spectra suggests its structure to include 5+4 bicyclic system. Then the most important

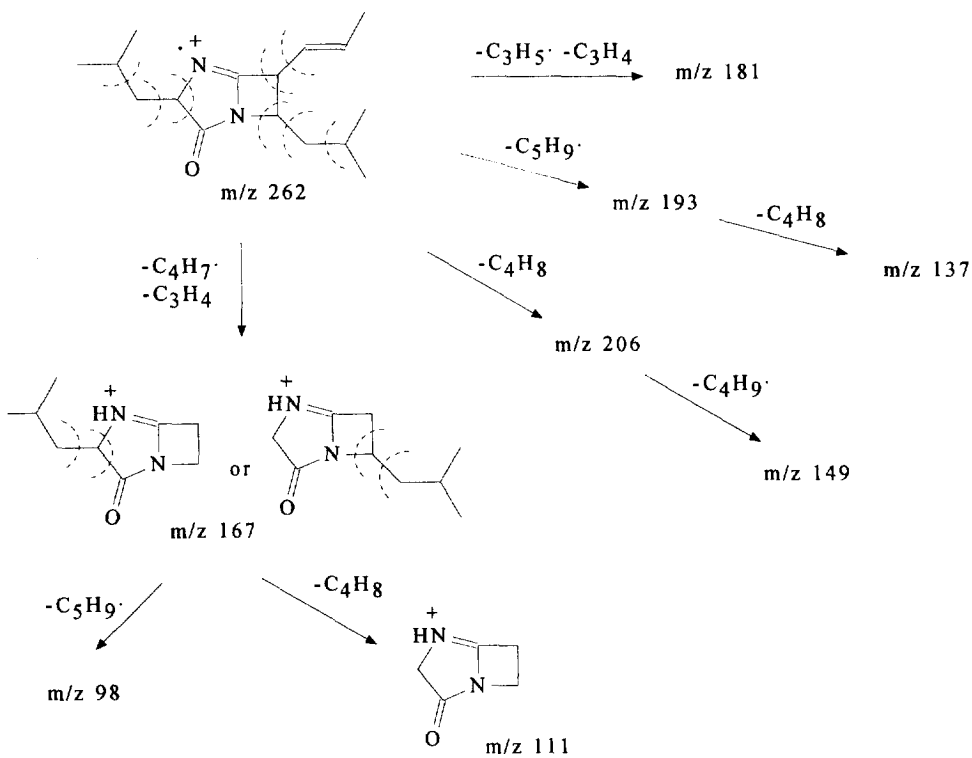

Fig. 12. EI fragmentation pattern for the compound **Leu-6**.

fragments in the **Leu-4** mass spectrum can be explained by the loss of C_4H_8 (*m/z* 111), $C_5H_9\cdot$ (*m/z* 98) and $C_5H_9(CO)\cdot$ (*m/z* 70).

Among all the detected and identified compounds, the most unexpected appears the component **Leu-3** for the following reason. Along with two very close $\nu_{C=O}$ bands at 1700–1750 cm^{-1}, it has a very sharp "nitrile" band ($\nu_{C\equiv N}$) at about 2250 cm^{-1} (Fig. 10). An even molecular mass (112) suggests only two nitrogen atoms to be present in the molecule. With such molecular mass and structural elements, the number of choices was very small, and we identified **Leu-3** as N-(cyanoformyl)acetamide. One should note that the PM3 calculations do not provide realistic intensity for the $\nu_{C\equiv N}$ band: compared to the experimental one, it appears lowered by approximately one order of magnitude.

The EI-MS and FTIR spectra of the compound **Leu-2** coincided totally with the spectra of tentatively identified amide **Val-3** (Fig. 8).

The component **Leu-1** of the lowest retention time (Fig. 9) has only one very intense $\nu_{C=O}$ band and no ν_{NH} band in its FTIR spectrum (Fig. 10). The compound has an even molecular mass number (144), but it seems quite unlikely to have two N atoms in the molecule. The fragmentation pattern has a series of ions at *m/z* 43, 57, 69 and 85 which may be attributed to the hydrocarbon series of $C_3H_7^+$, $C_4H_9^+$, $C_5H_9^+$ and $C_6H_{13}^+$. Based on the latter and on the comparison of the FTIR spectrum measured with spectra available in the literature [19] we conclude that **Leu-1** is a hexylacetate (structure of the hexyl residue is uncertain). The mechanism of its formation remains unclear.

Are the detected BCAs and TCAs just minor impurities in the products of silica-catalyzed amino acid condensation or they represent an important reaction pathway? A crude estimate of the amidine content based on peak intensities in the GC and HPLC chromatograms suggests that CHEs contain on average about 50% of BCAs, i.e., the total yields are 4 (Aib and Val) to 22% (Ala). Actually their yields due to the silica-catalyzed condensation are higher (roughly, twice higher), accounting for the degradation products. Thus BCAs indeed can represent a major reaction pathway for the amino acid transformations. At the same time, TCAs form as a whole in trace amounts.

Finally, it is interesting to evaluate briefly the prospect of utilizing computer simulation of IR spectra (in particular, by the PM3 method) to aid the interpretation of experimental FTIR data. As can be seen from the presented data, the general views of the calculated and experimental IR spectra look very similar. In addition, it is reasonable to analyze interrelation between the calculated and experimental wavenumbers for stretching vibrations in the amidines **Aib-3**, **Aib-4**, **Ala-2** and **Ala-3**, in the most important range of 1600–1800 cm^{-1} (stretching vibrations of the double bonds C=O, C=N and C=C). Within it, a linear interrelation between the calculated and experimental wavenumbers can be observed (Fig. 13). As mentioned before, the shift to higher wavenumbers by about 10% in this range is common for the semi-empirical method PM3 [18], as well as for the ab initio methods like MP2, CPF, SCF, etc. [20–27]. For ν_{CH} frequencies (around 3000 cm^{-1}), the simulation gives less than 5% deviation from the experimental values; here the shift can be to either higher or lower wavenumbers. For ν_{NH} vibrations (the range of 3400–3600 cm^{-1}), the calculated values appear to be lower than the experimental ones by about 50 cm^{-1}. Thus, the PM3 simulation of IR spectra in the spectral region of double bonds' stretching vibrations can be considered as a useful auxiliary tool for GC–FTIR identification of unknown carbonyl (particularly amide) compounds.

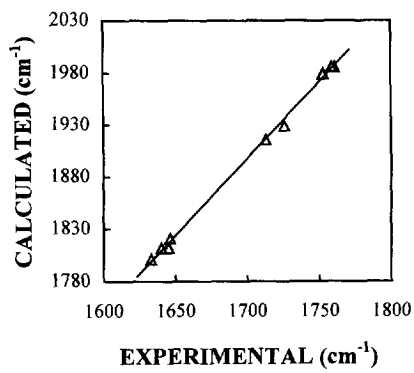

Fig. 13. Inter-relation between the calculated and experimental wavenumbers for the most important vibrations ($\nu_{C=O}$ and $\nu_{C=N}$) in BCAs and TCAs derived from Ala and Aib.

4. Conclusions

Sublimation of simple aliphatic amino acids (Ala, Aib, Val and Leu) at 230–250°C under reduced pressure in the presence of silica as a catalyst yielded PDs as major products (35–59%). In addition, mixtures of less-polar compounds have been separated from PDs by chloroform extraction. Using a coupled HPLC–PB-MS and GC–FTIR–MS technique with auxiliary computer simulation of IR spectra, we identified in the mixtures unusual products of amino acid condensation, namely substituted bicyclic and tricyclic amidines (hexahydroimidazo[1,2-*a*]pyrazine-3,6-diones and hexahydroimidazo[1,2-*a*]imidazo - [1,2-*d*]pyrazine-3,8-diones, respectively). Besides the amidines themselves, several products of their in situ thermal decomposition have been detected and identified by GC–FTIR–MS. The general decomposition pattern includes dehydrogenation as well as cleavage of the carbon skeleton. The imidazole ring appears to be more resistant to thermal decomposition as compared to the pyrazine moiety, so that the decomposition primarily affects the 6-membered pyrazine ring with elimination of CO or HNCO, or/and the loss of α-substituents without or with α-carbon atom itself, giving rise to the formation of different substituted imidazolones.

Acknowledgments

This work was supported by grants from the National Council of Science and Technology of Mexico (CONACyT-1843-OE9211, -F323E-9211 and -4282-E9406) and the National Autonomous University of Mexico (DGAPA-IN100393 and -IN102796).

References

[1] C.A. Bruckner, M.D. Foster, L.R. Lima, R.E. Synovec, R.J. Berman, C.N. Renn, E.L. Johnson, Anal. Chem. 66 (1994) 1R.
[2] G.A. Eiceman, H.H. Hill, B. Davani, Anal. Chem. 66 (1994) 621R.
[3] M.L. McKelvy, T.R. Britt, B.L. Davis, J.K. Gillie, L.A. Lentz, A. Leugers, R.A. Nyquist, C.L. Putzig, Anal. Chem. 68 (1996) 93R.
[4] G.A. Eiceman, H.H. Hill, B. Davani, J. Gardea-Torresday, Anal. Chem. 68 (1996) 291R.
[5] L.D. Rothman, Anal. Chem. 68 (1996) 587R.
[6] T.O. Munson, J. Vick, J. Anal. Appl. Pyrol. 8 (1985) 493.
[7] J.J. Boon, J.W. De Leeuw, J. Anal. Appl. Pyrol. 11 (1987) 313.
[8] T.O. Munson, D.D. Fetterolf, J. Anal. Appl. Pyrol. 11 (1987) 15.
[9] G.G. Smith, G.S. Reddy, J.J. Boon, J. Chem. Soc., Perkin Trans. 2 (1988) 203.
[10] A.S. Noguerola, B. Murugaverl, K.J. Voorhees, J. Am. Soc. Mass Spectrom. 3 (1992) 751.
[11] K.J. Voorhees, W. Zhang, A.D. Hendricker, B. Murugaverl, J. Anal. Appl. Pyrol. 30 (1994) 1.
[12] V.A. Basiuk, T.Yu. Gromovoy, A.A. Chuiko, V.A. Soloshonok, V.P. Kukhar, Synthesis (1992) 449.
[13] D. Gross, G. Grodsky, J. Am. Chem. Soc. 77 (1955) 1678.
[14] A. Ballistreri, M. Giuffrida, P. Maravigna, G. Montaudo, J. Polym. Sci. Polym. Chem. Ed. 23 (1985) 1145.
[15] D.S. Jones, G.W. Kenner, J. Preston, R.C. Sheppard, Tetrahedron 21 (1965) 3209.
[16] M.Y. Ali, J. Dale, K. Titlestad, Acta Chem. Scand. 27 (1973) 1509.
[17] M.Y. Ali, A. Khatun, Tetrahedron 41 (1985) 451.
[18] D.M. Seeger, C. Korzeniewski, W. Kowalchyk, J. Phys. Chem. 95 (1991) 6871.
[19] C.J. Pouchert, The Aldrich Library of FT-IR Spectra, Vol. 3, Vapor Phase, Aldrich, Milwaukee, WI, 1989.
[20] M.T. Ngugen, E. Van Praet, L.G. Vanquickenborne, Inorg. Chem. 33 (1994) 1153.
[21] H.S. Plitt, M.R. Bar, R. Ahlrichs, H. Schnockel, Inorg. Chem. 31 (1992) 463.
[22] H. Schnockel, T. Mehner, H.S. Plitt, S. Schunck, J. Am. Chem. Soc. 111 (1989) 4578.
[23] G.A. Arguello, B. Julicher, S.E. Ulic, H. Willner, B. Casper, H.-G. Mack, H. Oberhammer, Inorg. Chem. 34 (1995) 2089.
[24] S. Sieber, P. Von Rague Schleyer, H. Vancik, M. Mesic, D.E. Sunko, Angew. Chem. 32 (1993) 1604.
[25] G. Bucher, W. Sander, E. Kraka, D. Cremer, Angew. Chem. 31 (1992) 1230.
[26] T.-K. Ha, C. Pal, P.N. Ghosh, Spectrochim. Acta 48A (1992) 1083.
[27] E. Fjogstad, M. Ystenes, Spectrochim. Acta 46A (1990) 47.